Supplementary materials

A natural point mutation in the bitter taste receptor TAS2R16 causes inverse agonism of arbutin in lemur gustation

Akihiro Itoigawa, Takashi Hayakawa, Nami Suzuki-Hashido, Hiroo Imai

PROCEEDINGS OF THE ROYAL SOCIETY B
DOI: 10.1098/rspb.2019.0884

The table of contents

Supplementary methods

Cell culture and transfection

Human embryonic kidney 293T (HEK293T) cells were cultured in a 5% CO2 incubator at 37°C in Dulbecco's modified Eagle's medium (Sigma-Aldrich) supplemented with 10% foetal bovine serum (Sigma-Aldrich). The expression vector of TAS2R16 was transfected into HEK293T cells with Gα16/gust44 [1] using Lipofectamine 2000 (Thermo Fisher Scientific, Waltham, MA).

Calcium assay

Transfected cells were transferred to a 96-well Black with Clear Flat Bottom Corning CellBIND Surface plate (Corning, Inc., Corning, NY) 6 h after transfection. The cells were incubated for 16–18 h, rinsed with assay buffer (130 mM NaCl, 10 mM glucose, 5 mM KCl, 2 mM $CaCl_2$, 1.2 mM $MgCl_2$, 10 mM HEPES, pH 7.4), supplemented with 100 µl of Calcium 4 (Molecular Devices, Sunnyvale, CA) diluted two-fold with assay buffer as a calcium indicator, and incubated for 40 min at 27°C. Fluorescence at 525 nm following excitation at 485 nm was measured at 2-s intervals for 120 s at 27°C using FlexStation3 (Molecular Devices). Background fluorescence was measured for the first 20 s, then 100 µl of 2× test compound solution was added, and scanning was continued for an additional 100 s. Final concentrations of salicin and phenyl β-d-glucopyranoside (β-glucoside #1) were set to 0, 0.25, 1, 2.5, 5, 10, 20, and 40 mM, and those of arbutin, 4-nitrophenyl β-d-glucopyranoside (β-glucoside #2), and 4-methoxyphenyl β-d-glucopyranoside (β-glucoside #3) were set to 0, 0.25, 1, 2.5, 5, and 10 mM. Data were collected from 3–4 independent experiments. The calcium response is expressed as the normalised peak response (F) relative to background fluorescence (F_0): $\Delta F/F$ (= $[F- F_0]/F_0$). The response of cells transfected with the empty pEAK10 vector (no insert) and Gα16/gust44 was defined as the TAS2R-indipendent response and was subtracted from all responses. ΔF/F values were fitted to the nonlinear regression model ($y = \min + [(\max - \min)/(1 + x/EC_{50})^h]$), where x is the test compound concentration and h is the Hill coefficient. EC_{50} values and IC_{50} values were estimated by nonlinear regression model fitting using the drc package in R [2] and were compared among species by one-way ANOVA followed by Welch's tests with the BH correction.

IP_1 assay

Because IP_3 (inositol triphosphate), the second messenger of TAS2Rs, is quite short-lived, inositol dephosphorylation was stopped at IP_1 (inositol phosphate), a metabolite of IP_3, by adding LiCl; the concentration of accumulated IP_1 was measured by an immunoassay using the IP-One-Gq Kit (Cisbio, Codolet, France). Transfected cells were transferred to a 384-well plate (Greiner, Monroe, NC) 6 h after transfection. The cells were incubated for 12–14 h, rinsed with Stimulation Buffer, supplemented with 20 µl of Stimulation Buffer from the IP-One-Gq Kit and supplemented with 8 µl of 3.5× arbutin solution or Stimulation Buffer. After 60 min of incubation at 37°C in a 5% CO_2 incubator, the cells were supplemented with 4 µl of d2-conjugated IP_1 and Tb cryptate-conjugated anti-IP_1 antibodies, both from the IP-One-Gq Kit, and prepared in the cell lysis buffer supplied in the kit. After 60 min of incubation at room temperature, plates were read on the FlexStation3 using a fluorescence ratio (668 nm/620 nm), and the fluorescence ratio was converted to the IP_1 concentration using the standard curve generated from known concentrations of IP_1. Data were collected from 7–8 independent experiments. IP_1 production was compared among species and concentrations by Welch's tests with the BH correction.

Identification of TAS2R16 orthologues from the genome assemblies

To identify *TAS2R16* orthologues from the genome assemblies, a blastn search was performed using BLAST 2.8.0+ [3]. Reciprocal blastn against the human genome assembly GRCh38.p7 was performed to confirm whether the identified sequences are *TAS2R16* orthologues. The open reading frames with minimal flanking sequences were evaluated using TOPCONS [4] for the presence of seven transmembrane domains.

Structure modelling of lemur TAS2R16 and ligand docking into lemur TAS2R16

The three-dimensional structure of lemur TAS2R16 was predicted by the homology modelling method. A human TAS2R16 structure model constructed by the GPCR-I-TASSER server [5] was used as a template. A multiple sequence alignment of human, black lemur, ruffed lemur, and ring-tailed lemur TAS2R16 was generated using MAFFT [6] and then individual lemur TAS2R16 structure models were constructed using MODELLER [7]. Molecular docking simulations were performed using the rDock programme (http://rdock.sourceforge.net/) [8]. Owing to similarity in the shape of the agonist binding site among structure models of black lemur, ruffed lemur, and ring-tailed lemur TAS2R16

(figure S8), the model of black lemur TAS2R16 was selected as a representative lemur TAS2R16 structure and used for ligand docking. Based on the putative agonist binding site of human TAS2R16 [9], the ligand-binding site was defined to include all atoms within 10 Å of the midpoint between Trp85 Cα and His181 Cα atoms, and arbutin and salicin were docked into this site to generate fifty docking poses per ligand. After the docking structure models were energy-minimised using the minab module in the Amber12 package [10], the protein-ligand binding stability was assessed by the Molecular Mechanics Poisson-Boltzmann Surface Area (MM-PBSA) scoring [11,12] using the MMPBSA.py module [13] in the same package. Ionic strength was set to 150 mM. The top-ranked docking poses were used to represent the ligand-binding mode.

References

1. Ueda T, Ugawa S, Yamamura H, Imaizumi Y, Shimada S. 2003 Functional interaction between T2R taste receptors and G-protein alpha subunits expressed in taste receptor cells. *J. Neurosci.* **23**, 7376–7380. (doi:10.1523/JNEUROSCI.23-19-07376.2003)
2. Ritz C, Baty F, Streibig JC, Gerhard D. 2015 Dose-response analysis using R. *PLoS One* **10**, 1–13. (doi:10.1371/journal.pone.0146021)
3. Altschul SF, Madden TL, Schäffer AA, Zhang J, Zhang Z, Miller W, Lipman DJ. 1997 Gapped BLAST and PSI-BLAST:a new generation of protein database search programs. *Nucleic Acids Res.* **25**, 3389–3402. (doi:10.1093/nar/25.17.3389)
4. Tsirigos KD, Peters C, Shu N, Käll L, Elofsson A. 2015 The TOPCONS web server for consensus prediction of membrane protein topology and signal peptides. *Nucleic Acids Res.* **43**, W401–W407. (doi:10.1093/nar/gkv485)
5. Zhang J, Yang J, Jang R, Zhang Y. 2015 GPCR-I-TASSER : A Hybrid Approach to G Protein- Coupled Receptor Structure Modeling and the Application to the Human Genome Resource. *Structure* **23**, 1538–1549. (doi:10.1016/j.str.2015.06.007)
6. Katoh K, Standley DM. 2013 MAFFT multiple sequence alignment software version 7: Improvements in performance and usability. *Mol. Biol. Evol.* **30**, 772–780. (doi:10.1093/molbev/mst010)
7. Sali A, Blundell TL. 1993 Comparative Protein Modelling by Satisfaction of Spatial Restraints. *J. Mol. Biol.* **234**, 779–815. (doi:10.1006/jmbi.1993.1626)
8. Ruiz-Carmona S, Alvarez-Garcia D, Foloppe N, Garmendia-doval AB, Juhos S, Schmidtke P, Barril X, Hubbard RE, Morley SD. 2014 rDock: A Fast, Versatile and Open Source Program for Docking Ligands to Proteins and Nucleic Acids. *PLoS Comput. Biol*. **10**, e1003571. (doi:10.1371/journal.pcbi.1003571)
9. Sakurai T *et al*. 2010 Characterization of the β-D-Glucopyranoside binding site of the human bitter taste receptor hTAS2R16. *J. Biol. Chem.* **285**, 28373–28378. (doi:10.1074/jbc.M110.144444)
10. Case DA *et al*. 2012 AMBER 12.
11. Massova I, Kollman PA. 1999 Computational Alanine Scanning To Probe Protein - Protein Interactions : A Novel Approach To Evaluate Binding Free Energies. *J. Am. Chem. Soc.* **121**, 8133–8143. (doi:10.1021/ja990935j)
12. Kollman PA et al. 2000 Calculating Structures and Free Energies of Complex Molecules : Combining Molecular Mechanics and Continuum Models. Acc. *Chem. Res*. **33**, 889–897. (doi:10.1021/ar000033j)
13. Miller, III BR, McGee, Jr. TD, Swails JM, Homeyer N, Gohlke H, Roitberg AE. 2012 MMPBSA.py: An Efficient Program for End-State Free Energy Calculations. *J. Chem. Theory Comput*. **8**, 3314–3321. (doi:10.1021/ct300418h)

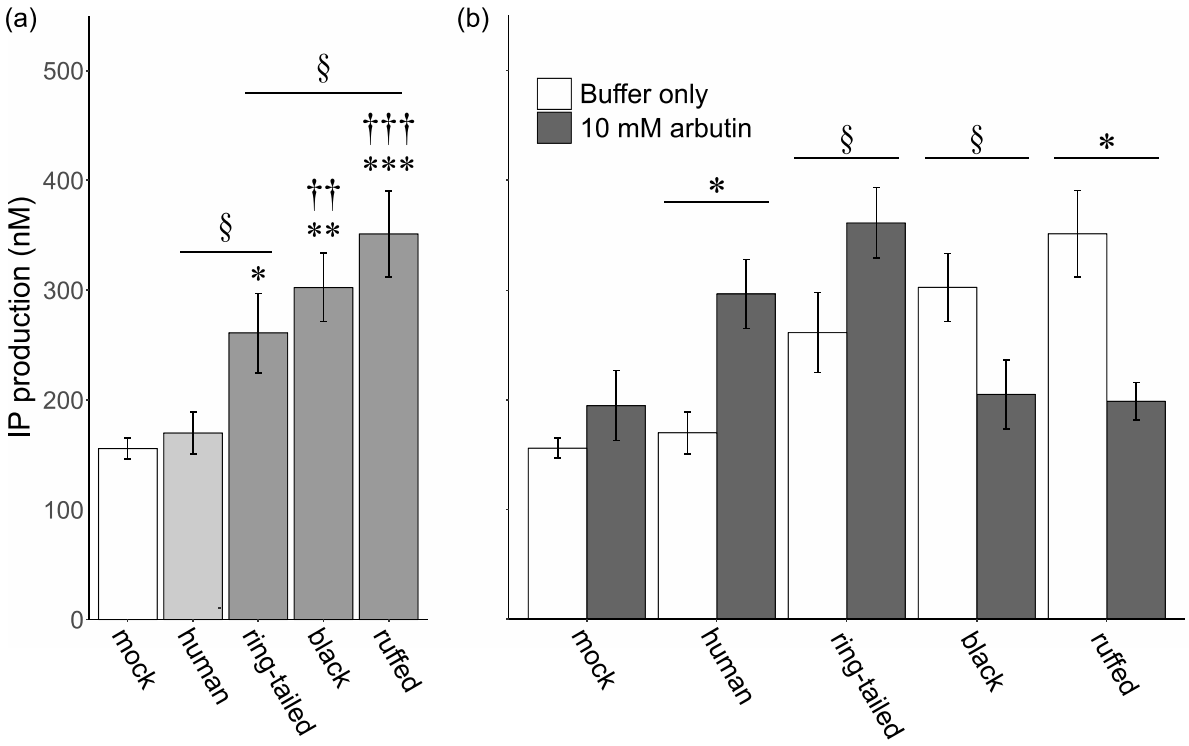

Figure S1. Lemurs showed high basal IP_1 production.
(a) HEK293T cells expressing TAS2R16 of each lemur or empty pEAK10 (mock) with Gα16/gust44 were stimulated with assay buffer for 60 min. IP_1 production was calculated using standard curves generated using known concentrations of IP_1. Significant differences were determined by one-way ANOVA followed by Welch's tests with the BH correction (FDR q-value, *: $P < 0.05$, **: $P < 0.01$, ***: $P < 0.001$ for mock, †: $P < 0.05$, ††: $P < 0.01$, †††: $P < 0.001$ for human, §: $P < 0.1$). (b) HEK293T cells expressing TAS2R16 of each lemur or empty pEAK10 (mock) with Gα16/gust44 were stimulated with 10 mM arbutin or assay buffer for 60 min. IP_1 production was calculated using standard curves generated from known concentrations of IP_1. Significant differences between buffer and arbutin in each species were determined by one-way ANOVA followed by Welch's tests with the BH correction (FDR q-value, §: $P < 0.1$, *: $P < 0.05$, **: $P < 0.01$, ***: $P < 0.001$).

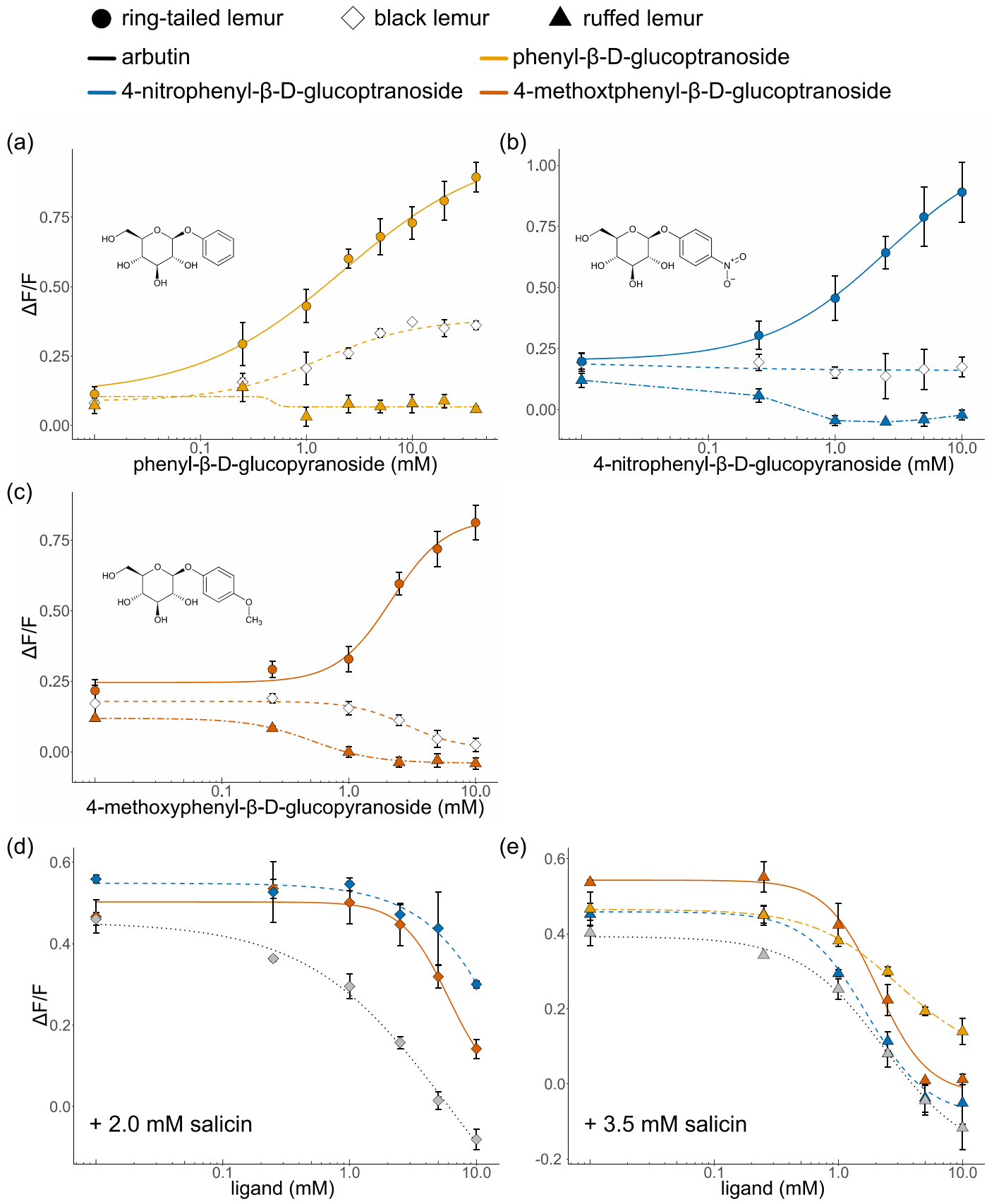

Figure S2. Differences in responses to arbutin analogues among species.
HEK293T cells expressing TAS2R16 of each lemur with Gα16/gust44 were stimulated with increasing concentrations of (a) phenyl β-d-glucopyranoside (β-glucoside #1), (b) 4-nitrophenyl β-d-glucopyranoside (β-glucoside #2) and (c) 4-methoxyphenyl β-d-glucopyranoside (β-glucoside #3). (d) HEK293T cells expressing the TAS2R16 of black lemur with Gα16/gust44 were stimulated with increasing concentrations of arbutin, β-glucoside #2 and β-glucoside #3 in presence of 2.0 mM salicin. (e) HEK293T cells expressing the TAS2R16 of ruffed lemur with Gα16/gust44 were stimulated with increasing concentrations of arbutin, β-glucoside #1, β-glucoside #2 and β-glucoside #3 in presence of 3.5 mM salicin. Changes in fluorescence (ΔF/F) upon ligand application were monitored (mean ± SEM). Experiments were performed 3–4 times independently.

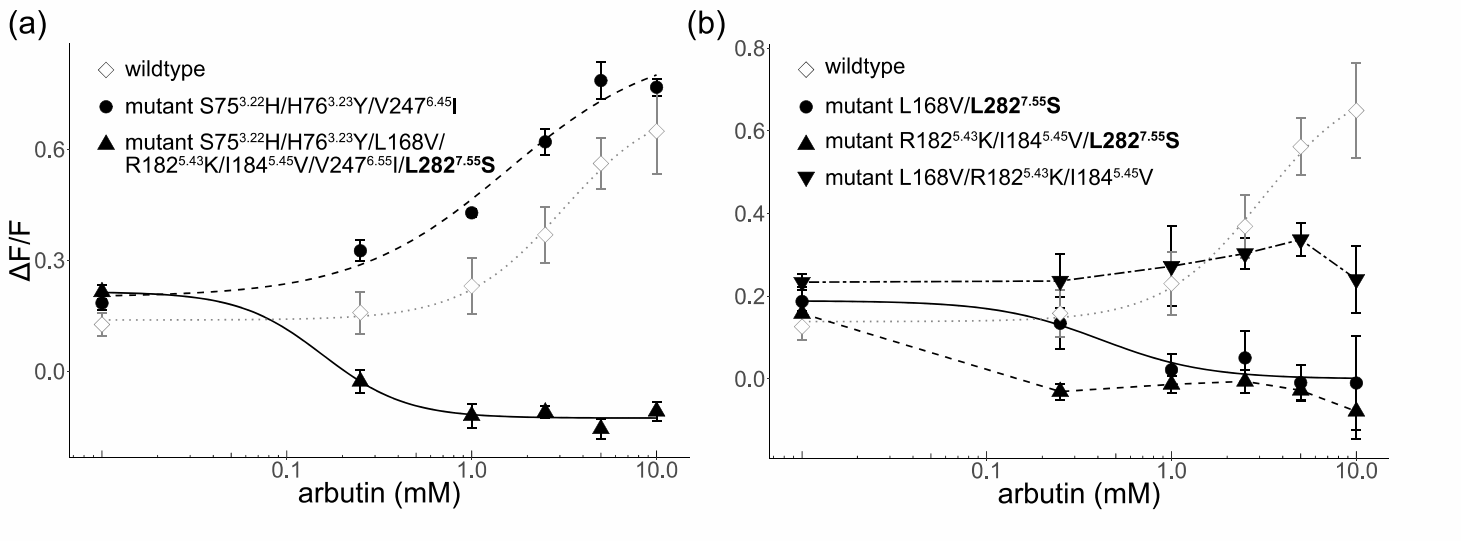

Figure S3. Screening of the amino acid position responsible for arbutin recognition in ring-tailed lemur TAS2R16.

HEK293T cells expressing TAS2R16 of ring-tailed lemur or its mutants with Gα16/gust44 were stimulated with increasing concentrations of arbutin. Changes in fluorescence (ΔF/F) upon ligand application were monitored (mean ± SEM). Experiments were performed 3–4 times independently. The 7-site mutant TAS2R16 of the ring-tailed lemur (S75$^{3.22}$N/H76$^{3.23}$Y/L168V/R182$^{5.43}$K/I184$^{5.45}$V/V247$^{6.55}$I/L282$^{7.55}$S) and 3-site mutant (S75$^{3.22}$H/H76$^{3.23}$Y/V247$^{6.55}$I) are shown in (a). Mutants with substitutions at four candidate amino acid positions (L168V/R182$^{5.43}$K/I184$^{5.45}$V/L282$^{7.55}$S) are shown in (b).

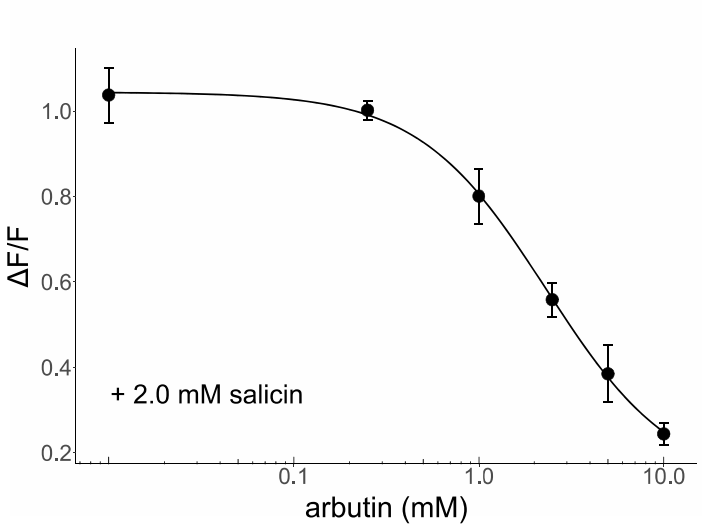

Figure S4. Arbutin inhibited the salicin-mediated activation of TAS2R16 in the 282$^{7.55}$ residue-mutant of the ring-tailed lemur.
HEK293T cells expressing the TAS2R16 mutant of ring-tailed lemur with a substitution at position 282$^{7.55}$ with Gα16/gust44 were stimulated with increasing concentrations of arbutin in presence of 2.0 mM salicin. Changes in fluorescence (ΔF/F) upon ligand application were monitored (mean ± SEM). Experiments were performed 3–4 times independently.

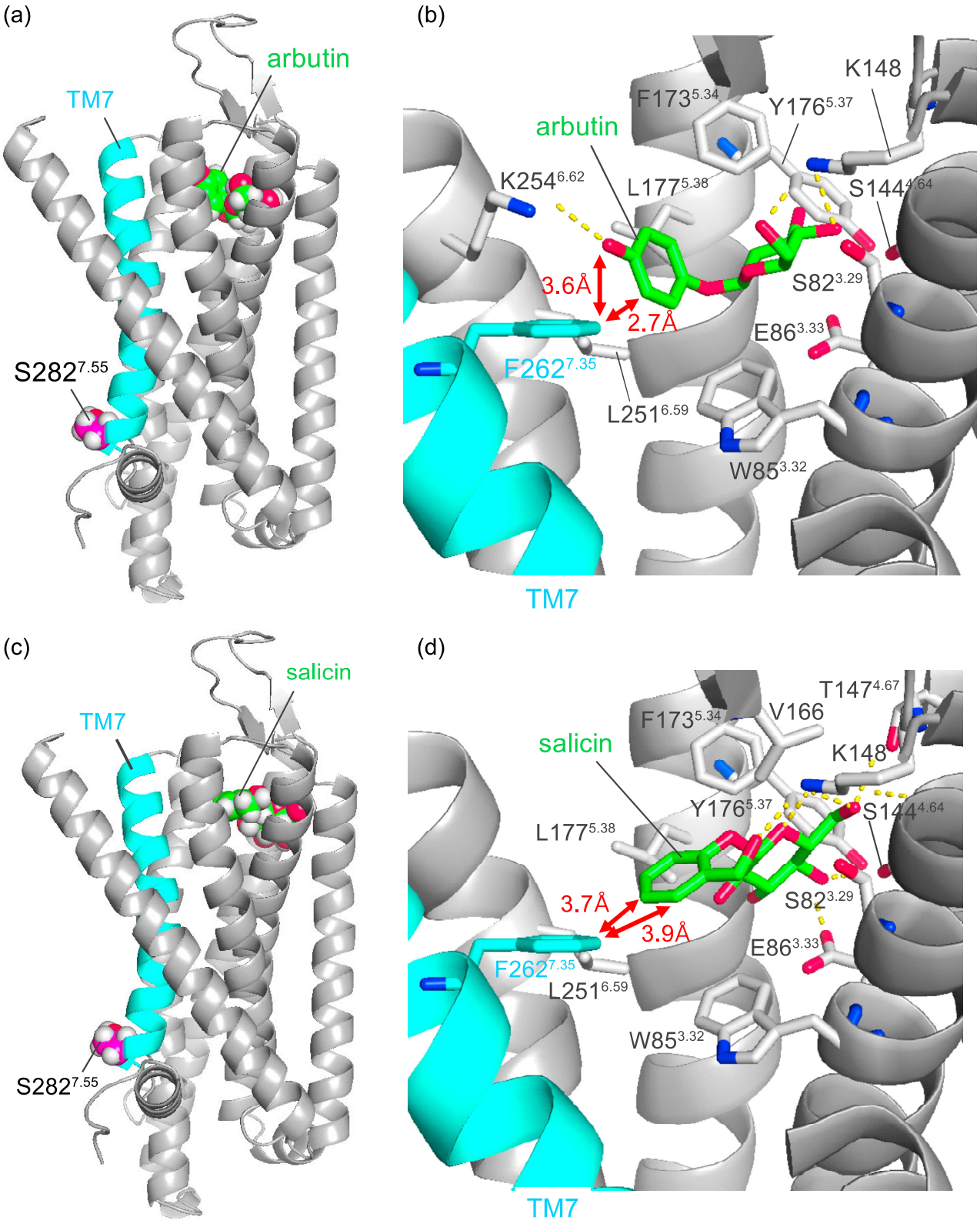

Figure S5. Predicted ligand-binding mode for lemur TAS2R16.
(a and c) Overall structure of black lemur TAS2R16. The protein backbone structure is depicted by a grey ribbon diagram, and transmembrane helix 7 (TM7) is highlighted in cyan. The side chain of S282$^{7.55}$, (a) arbutin and (c) salicin are represented by spheres (magenta/green, carbon; blue, nitrogen; red, oxygen, white; hydrogen). (b and d) A close-up view of the ligand binding site. (b) Arbutin, (d) salicin and amino acid residues located within 3Å from the ligand are represented by sticks. Receptor-ligand hydrogen bonds are indicated by yellow dashed lines.

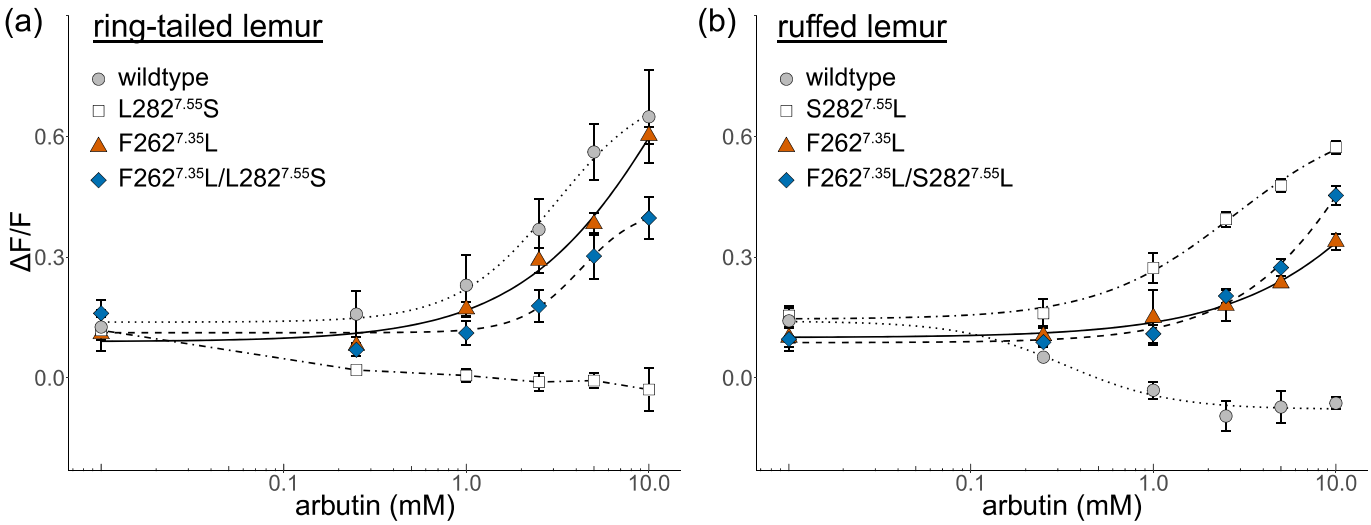

Figure S6. Position $262^{7.35}$ is related to the activation of lemur TAS2R16s.
Mutant TAS2R16 of (a) the ring-tailed lemur and (b) ruffed lemur at position $262^{7.35}$ and $282^{7.55}$ were stimulated with increasing concentrations of arbutin. Changes in fluorescence (ΔF/F) were monitored (mean ± SEM). Experiments were performed 3–5 times independently.

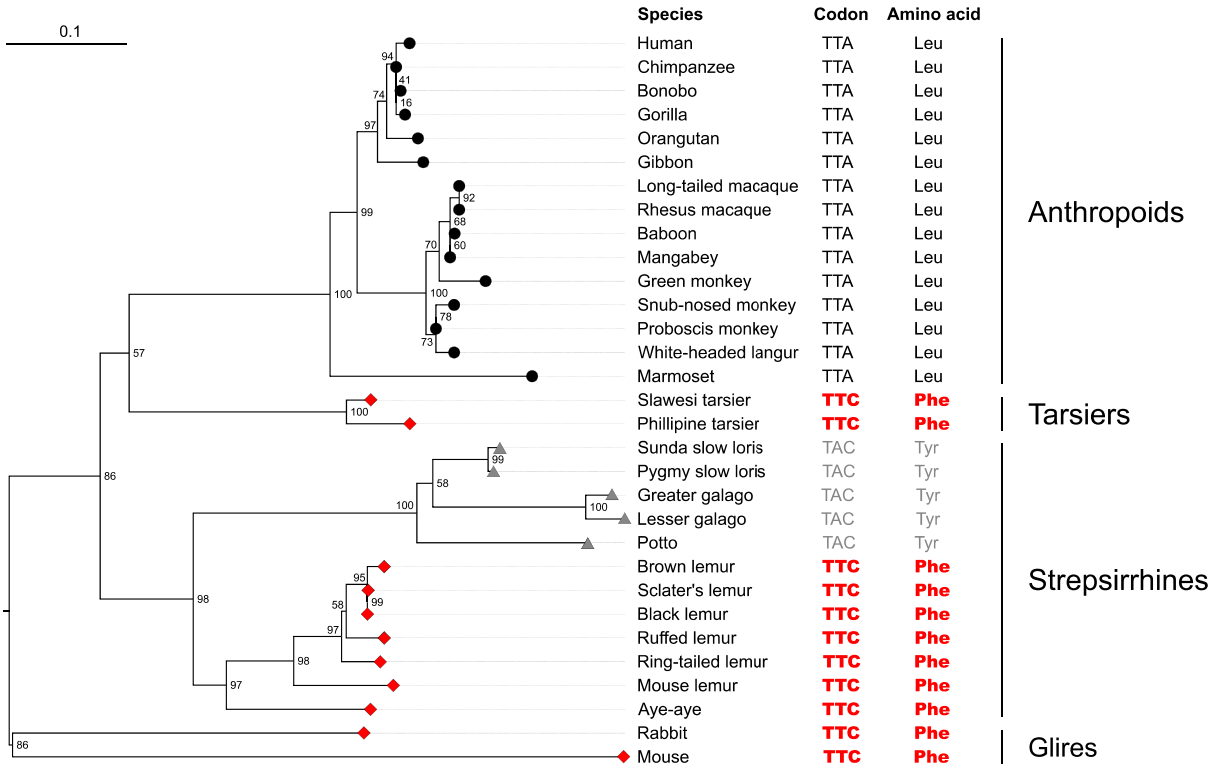

Figure S7. Evolutionary history of the amino acid residue at position 262$^{7.35}$ in TAS2R16. Maximum likelihood tree was reconstructed based on the amino acid sequences of TAS2R16 in primates. The amino acid residue at position 262$^{7.35}$ in each species is indicated at each tip of the tree (red diamonds indicate phenylalanine, black circles indicate leucine, grey triangles indicate tyrosine). Bootstrap values are expressed at the nodes of the tree. The amino acid residue at position 262$^{7.35}$ and the corresponding codon of primates are shown next to the species name.

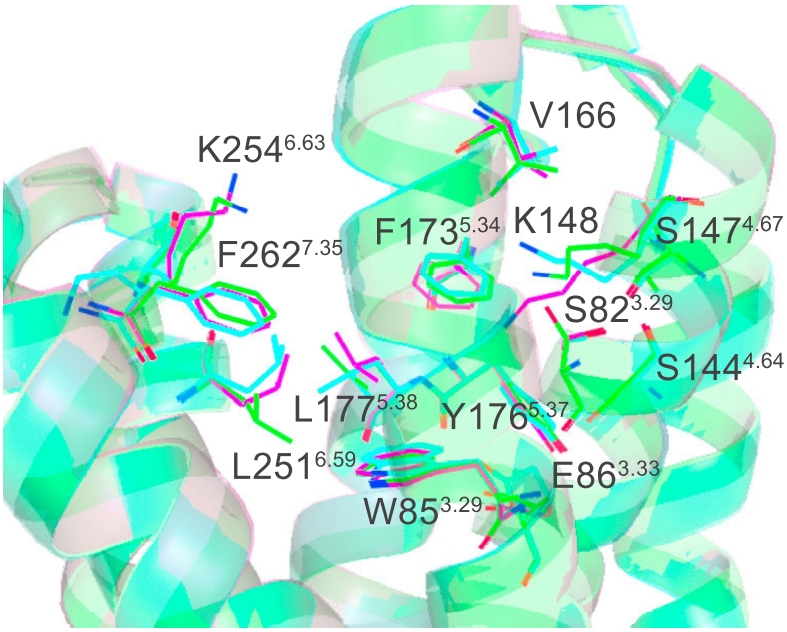

Figure S8. Superimposition of structure models of TAS2R16 of the three lemurs.
Superimposition of structure models of black lemur (green), ruffed lemur (cyan), and ring-tailed lemur (magenta) TAS2R16. Protein backbone structures are depicted by transparent ribbon diagrams, and amino acid residues forming the putative agonist binding site (Sakurai, T. et al., The Journal of biological chemistry 2010, 285 (36), 28373-8.) are represented by sticks (green/cyan/magenta, carbon; blue, nitrogen; red, oxygen), suggesting similarity of the pocket shape among these three receptors.

Table S1. Detailed information for the sources of genomic DNA and the subject of the behavioural assay

Genetic resource

Species	Scientific name	Provider	Individual	Sex	Tissue	Extraction kit
Ring-tailed lemur	*Lemur catta*	Japan Monkey Centre	Pr5862	Female	muscle	DNAeasy Blood &Tissue Kit
Black lemur	*Eulemur macaco*	Japan Monkey Centre	Pr6526	Female	muscle	DNAeasy Blood &Tissue Kit
Black-and-white ruffed lemur	*Varecia variegata*	Japan Monkey Centre	Pr5649	Female	muscle	DNAeasy Blood &Tissue Kit
Brown lemur	*Eulemur fulvus*	Japan Monkey Centre	Unknown	Unknown	faeces	QIAamp Fast DNA Stool Mini Kit
Sunda slow loris	*Nycticebus coucang*	Japan Monkey Centre	Pr6102	Female	muscle	DNAeasy Blood &Tissue Kit
Lesser slow loris	*Nycticebus pygmaeus*	Japan Monkey Centre	Pr6568	Male	muscle	DNAeasy Blood &Tissue Kit
Senegal lesser galago	*Galago senegalensis*	Japan Monkey Centre	Pr5790	Female	muscle	DNAeasy Blood &Tissue Kit
Potto	*Perodicticus potto*	Japan Monkey Centre	Pr6581	Male	muscle	DNAeasy Blood &Tissue Kit
Sulawesi tarsier	*Tarsius tarsier*	Ueno Zoological Gardens	Unknown	Unknown	faeces	NucleoSpin DNA Stool Kit

Behavioural assay

Species	Scientific name	Housing	Individual	Sex	Age
Black lemur	*Eulemur macaco*	Japan Monkey Centre	5278 ("San")	Female	over 20 yo

Table S2. Genome assemblies of placental mammals for identifying TAS2R16 genes

Name	Species	Assembly	Source *	Reference
Human	*Homo sapiens*	GRCh38.p12	NCBI	Genome Reference Consortium
Mangabey	*Cercocebus atys*	Caty_1.0	NCBI	[14]
Green monkey	*Chlorocebus sabaeus*	Chlorocebus_sabeus 1.1	NCBI	[15]
Snub-nosed monkey	*Rhinopithecus roxellana*	Rrox_v1	NCBI	[16]
Proboscis monkey	*Nasalis larvatus*	Chaelie1.0	NCBI	unpublished
Mouse lemur	*Microcebus murinus*	Mmur_3.0	NCBI	[17]
Sclater's lemur	*Eulemur flaviflons*	Eflavifronsk33QCA	NCBI	[18]
Flying lemur	*Galeopterus variegatus*	G_variegatus-3.0.2	NCBI	unpublished
Chinese tree shrew	*Tupaia chinensis*	TupChi_1.0	NCBI	[19]
Elephant	*Loxodonta africana*	Loxafr3.0	NCBI	[17]
Manatee	*Trichechus manatus*	TriManLat1.0	NCBI	[20]
Hyrax	*Procavia capensis*	Pcap_2.0	NCBI	[17]
Tenrec	*Echinops telfairi*	EchTel2.0	NCBI	[17]

* Web source: NCBI, National Center for Biotechnology Information (https://www.ncbi.nlm.nih.gov/).

References

14. Palesch D *et al.* 2018 Sooty mangabey genome sequence provides insight into AIDS resistance in a natural SIV host. *Nature* **553**, 77–81. (doi:10.1038/nature25140)
15. Warren WC *et al.* 2015 The genome of the vervet (Chlorocebus aethiops sabaeus). *Genome Res.* **25**, 1921–1933. (doi:10.1101/gr.192922.115)
16. Zhou X *et al.* 2014 Whole-genome sequencing of the snub-nosed monkey provides insights into folivory and evolutionary history. *Nat. Genet.* **46**, 1303–1310. (doi:10.1038/ng.3137)
17. Lindblad-Toh K *et al.* 2011 A high-resolution map of human evolutionary constraint using 29 mammals. *Nature* **478**, 476–482. (doi:10.1038/nature10530)
18. Meyer WK, Venkat A, Kermany AR, Van De Geijn B, Zhang S, Przeworski M. 2015 Evolutionary history inferred from the de novo assembly of a nonmodel organism, the blue-eyed black lemur. *Mol. Ecol.* **24**, 4392–4405. (doi:10.1111/mec.13327)
19. Fan Y *et al.* 2013 Genome of the Chinese tree shrew. *Nat. Commun.* **4**. (doi:10.1038/ncomms2416)
20. Foote AD *et al.* 2015 Convergent evolution of the genomes of marine mammals. *Nat. Genet.* **47**, 272–275. (doi:10.1038/ng.3198)

Table S3. Amino acid residues at position $262^{7.35}$ and $282^{7.55}$ of TAS2R16 orthologues in placental mammals

Species	Scientific name	Order	AA $262^{7.35}$	AA $282^{7.55}$	Accession number	References
Human	*Homo sapiens*	Primates	TTA/Leu	CTG/Leu		[21]
Chimpanzee	*Pan troglodytes verus*	Primates	TTA/Leu	CTG/Leu		[21]
Bonobo	*Pan panicus*	Primates	TTA/Leu	CTG/Leu		[21]
Gorilla	*Gorilla gorilla gorilla*	Primates	TTA/Leu	CTG/Leu		[21]
Orangutan	*Pongo abelii*	Primates	TTA/Leu	CTG/Leu		[21]
Gibbon	*Nomascus leucogenys*	Primates	TTA/Leu	CTG/Leu		[21]
Mangabey	*Cercocebus atys*	Primates	TTA/Leu	CTG/Leu	NW_012002290.1:21536045-21536920	[14]
Baboon	*Papio anubis*	Primates	TTA/Leu	CTG/Leu		[21]
Rhesus macaque	*Macaca mulatta*	Primates	TTA/Leu	CTG/Leu		[21]
Long-tailed macaque	*Macaca fascicularis*	Primates	TTA/Leu	CTG/Leu		[21]
Green monkey	*Chlorocebus sabaeus*	Primates	TTA/Leu	CTG/Leu	NC_023662.1:91783088-91783963	[15]
White-headed langur	*Trachypithecus leucocephalus*	Primates	TTA/Leu	CTG/Leu		[23]
Snub-nosed monkey	*Rhinopithecus roxellana*	Primates	TTA/Leu	CTG/Leu	NW_010807527.1:195193-196068	[16]
Proboscis monkey	*Nasalis larbatus*	Primates	TTA/Leu	CTG/Leu	CM003011.1:147496274-147497149	unpublished
Marmoset	*Callithrix jacchus*	Primates	TTA/Leu	CTG/Leu		[21]
Squirrel monkey *	*Saimiri boliviensis*	Primates	TTA/Leu	CTG/Leu		[21]
Sulawesi tarsier	*Tarsius tarsier*	Primates	TTC/Phe	CTG/Leu	DDBJ accession [LC415000]	this study
Philippine tarsier	*Calrito syricata*	Primates	TTC/Phe	CTG/Leu		[21]
Aye-aye	*Daubentonia madagascariensis*	Primates	TTC/Phe	**TCG/Ser**		[21]
Mouse lemur	*Microcebus murinus*	Primates	TTC/Phe	**TCG/Ser**	NW_012202341.1:735189-736094	[17]
Ruffed lemur	*Varecia variegata*	Primates	TTC/Phe	**TCG/Ser**	DDBJ accession [LC414993]	this study
Brown lemur	*Eulemur fulvus*	Primates	TTC/Phe	**TCG/Ser**	DDBJ accession [LC414995]	this study
Sclater's lemur	*Eulemur flaviflons*	Primates	TTC/Phe	**TCG/Ser**	LGHW01000662.1:100449-101354	[18]
Black lemur	*Eulemur macaco*	Primates	TTC/Phe	**TCG/Ser**	DDBJ accession [LC414994]	this study
Ring-tailed lemur	*Lemur catta*	Primates	TTC/Phe	**TTG/Leu**	DDBJ accession [LC414992]	this study
Sunda slow loris	*Nycticebus coucang*	Primates	TAC/Tyr	**TCG/Ser**	DDBJ accession [LC414997]	this study

Pygmy slow loris	*Nycticebus pygmaeus*	Primates	TAC/Tyr	**TCG/Ser**	DDBJ accession [LC414998]	this study
Potto	*Perodicticus potto*	Primates	TAC/Tyr	**TCG/Ser**	DDBJ accession [LC414996]	this study
Lesser galago	*Galago senegalensis*	Primates	TAC/Tyr	GCA/Ala	DDBJ accession [LC414999]	this study
Greater galago	*Otolemur garnettii*	Primates	TAC/Tyr	GCA/Ala		[21]
Flying lemur	*Galeopterus variegatus*	Dermoptera	TAC/Tyr	CTG/Leu	NW_007726231.1:755116-756025	unpublished
Chinese tree shrew	*Tupaia chinensis*	Scandentia	TTC/Phe	CTG/Leu	NW_006159737.1:2521943-2522848	[19]
Northern tree shrew	*Tupaia belangeri*	Scandentia	TTC/Phe	CTG/Leu		[21]
Mouse	*Mus musculus* strain C57BL/6J	Rodentia	TTC/Phe	ATG/Met		[21]
Rat	*Rattus norvegicus* strain BN	Rodentia	TTC/Phe	ATG/Met		[21]
Hamster	*Cricetulus griseus*	Rodentia	TTC/Phe	ATG/Met		[21]
Jerboa	*Jaculus jaculus*	Rodentia	TTT/Phe	CTG/Leu		[21]
Guinea pig	*Cavia porcellus*	Rodentia	TAC/Tyr	ATG/Met		[21]
Chinchilla	*Chinchilla lanigera*	Rodentia	TTC/Phe	CTG/Leu		[21]
Degu	*Octodon degus*	Rodentia	TCC/Ser	CTG/Leu		[21]
Naked mole rat	*Heterocephalus glaber*	Rodentia	TGC/Cys	CTG/Leu		[21]
Squirrel	*Ictidomys tridecemlineatus*	Rodentia	TAC/Tyr	CTG/Leu		[21]
Rabbit	*Oryctolagus cuniculus*	Lagomorpha	TTC/Phe	CTG/Leu		[21]
Przewalskis horse	*Equus ferus przewalskii*	Perissodactyla	TTC/Phe	CTG/Leu		[22]
Rhinoceros	*Ceratotherium simum*	Perissodactyla	TAC/Tyr	CTG/Leu		[22]
Minke whale	*Balaenoptera acutorostrata*	Cetartiodactyla	TTC/Phe	CTG/Leu		[22]
Wild goat	*Capra aegagrus*	Cetartiodactyla	TTC/Phe	CTG/Leu		[22]
Goat	*Capra aegagrus hircus*	Cetartiodactyla	TTC/Phe	CTG/Leu		[22]
Musimon	*Ovis aries musimon*	Cetartiodactyla	TTC/Phe	CTG/Leu		[22]
Sheep	*Ovis aries*	Cetartiodactyla	TTC/Phe	CTG/Leu		[22]
Yak	*Bos grunniens*	Cetartiodactyla	TTC/Phe	CTG/Leu		[22]
Tibetan antelope	*Pantholops hodgsonii*	Cetartiodactyla	TTC/Phe	CTG/Leu		[22]
Water buffalo	*Bubalus bubalis*	Cetartiodactyla	TTC/Phe	CTG/Leu		[22]
Zebu	*Bos indicus*	Cetartiodactyla	TTC/Phe	CTG/Leu		[22]

Cow	*Bos taurus*	Cetartiodactyla	TTC/Phe	CTG/Leu		[22]
Pig	*Sus scrofa*	Cetartiodactyla	TTC/Phe	CTG/Leu		[22]
Alpaca	*Vicugna pacos*	Cetartiodactyla	TTC/Phe	CTG/Leu		[22]
Big brown bat	*Eptesicus fuscus*	Chiroptera	TTC/Phe	CTG/Leu		[22]
Brandt's bat A	*Myotis brandtii*	Chiroptera	TTC/Phe	CTG/Leu		[22]
Brandt's bat B	*Myotis brandtii*	Chiroptera	TTC/Phe	CTG/Leu		[22]
Brandt's bat C	*Myotis brandtii*	Chiroptera	TTC/Phe	CTG/Leu		[22]
Brandt's bat D	*Myotis brandtii*	Chiroptera	TTC/Phe	CTG/Leu		[22]
David's myotis A	*Myotis davidii*	Chiroptera	TTC/Phe	CTG/Leu		[22]
David's myotis B	*Myotis davidii*	Chiroptera	TTC/Phe	CTG/Leu		[22]
David's myotis C	*Myotis davidii*	Chiroptera	TTC/Phe	CTG/Leu		[22]
Little brown bat A	*Myotis lucifugus*	Chiroptera	TTC/Phe	CTG/Leu		[22]
Little brown bat B	*Myotis lucifugus*	Chiroptera	TTC/Phe	CTG/Leu		[22]
Little brown bat C	*Myotis lucifugus*	Chiroptera	TTC/Phe	CTG/Leu		[22]
Little brown bat D	*Myotis lucifugus*	Chiroptera	TTC/Phe	CTG/Leu		[22]
Black flying fox	*Pteropus alecto*	Chiroptera	TTC/Phe	ATG/Met		[22]
Large flying fox	*Pteropus vampyrus*	Chiroptera	TTC/Phe	ATG/Met		[22]
Elephant	*Loxodonta africana*	Afrotheria	TTC/Phe	CTG/Leu	NW_003573425.1:92839824-92840705	[17]
Manatee	*Trichechus manatus*	Afrotheria	TTC/Phe	CTG/Leu	NW_004444103.1:1665079-1665963	[20]
Hyrax A	*Procavia capensis*	Afrotheria	TTC/Phe	CTG/Leu	KN676540.1:608280-609164	[17]
Hyrax C	*Procavia capensis*	Afrotheria	TTA/Leu	GCT/Ala	KN676540.1:640492-641421	[17]
Hyrax D	*Procavia capensis*	Afrotheria	TTC/Phe	CTG/Leu	KN676540.1:670412-671293	[17]
Hyrax E	*Procavia capensis*	Afrotheria	TTC/Phe	CTG/Leu	KN676540.1:691196-692077	[17]
Hyrax G	*Procavia capensis*	Afrotheria	TTC/Phe	CTA/Leu	KN676540.1:757022-757900	[17]
Hyrax H	*Procavia capensis*	Afrotheria	TTC/Phe	CTG/Leu	KN676540.1:767557-768441	[17]
Hyrax I	*Procavia capensis*	Afrotheria	TTC/Phe	CTG/Leu	KN676540.1:810168-811088	[17]
Hyrax J	*Procavia capensis*	Afrotheria	TTC/Phe	CTG/Leu	KN676540.1:814538-815458	[17]
Hyrax K	*Procavia capensis*	Afrotheria	TTC/Phe	CTG/Leu	KN676540.1:822452-823336	[17]

Tenrec	*Echinops telfairi*	Afrotheria	TTC/Phe	CTG/Leu	NW_004558729.1:15899598-15900497	[17]

* TAS2R16 of Squirrel monkey was pseudogenized.

References

14. Palesch D *et al.* 2018 Sooty mangabey genome sequence provides insight into AIDS resistance in a natural SIV host. *Nature* **553**, 77–81. (doi:10.1038/nature25140)
15. Warren WC *et al.* 2015 The genome of the vervet (Chlorocebus aethiops sabaeus). *Genome Res.* **25**, 1921–1933. (doi:10.1101/gr.192922.115)
16. Zhou X *et al.* 2014 Whole-genome sequencing of the snub-nosed monkey provides insights into folivory and evolutionary history. *Nat. Genet.* **46**, 1303–1310. (doi:10.1038/ng.3137)
17. Lindblad-Toh K *et al.* 2011 A high-resolution map of human evolutionary constraint using 29 mammals. *Nature* **478**, 476–482. (doi:10.1038/nature10530)
18. Meyer WK, Venkat A, Kermany AR, Van De Geijn B, Zhang S, Przeworski M. 2015 Evolutionary history inferred from the de novo assembly of a nonmodel organism, the blue-eyed black lemur. *Mol. Ecol.* **24**, 4392–4405. (doi:10.1111/mec.13327)
19. Fan Y *et al.* 2013 Genome of the Chinese tree shrew. *Nat. Commun.* **4**. (doi:10.1038/ncomms2416)
20. Foote AD *et al.* 2015 Convergent evolution of the genomes of marine mammals. *Nat. Genet.* **47**, 272–275. (doi:10.1038/ng.3198)
21. Hayakawa T, Suzuki-Hashido N, Matsui A, Go Y. 2014 Frequent expansions of the bitter taste receptor gene repertoire during evolution of mammals in the euarchontoglires clade. *Mol. Biol. Evol.* **31**, 2018–2031. (doi:10.1093/molbev/msu144)
22. Liu Z, Liu G, Hailer F, Orozco-terWengel P, Tan X, Tian J, Yan Z, Zhang B, Li M. 2016 Dietary specialization drives multiple independent losses and gains in the bitter taste gene repertoire of Laurasiatherian Mammals. *Front. Zool.* **13**, 28. (doi:10.1186/s12983-016-0161-1)
23. Imai H, Suzuki N, Ishimaru Y, Sakurai T, Yin L, Pan W, Abe K, Misaka T, Hirai H. 2012 Functional diversity of bitter taste receptor TAS2R16 in primates. *Biol. Lett.* **8**, 652–656. (doi:10.1098/rsbl.2011.1251)

Table S4. Amino acid sequences of TAS2R16 in human and three lemurs.

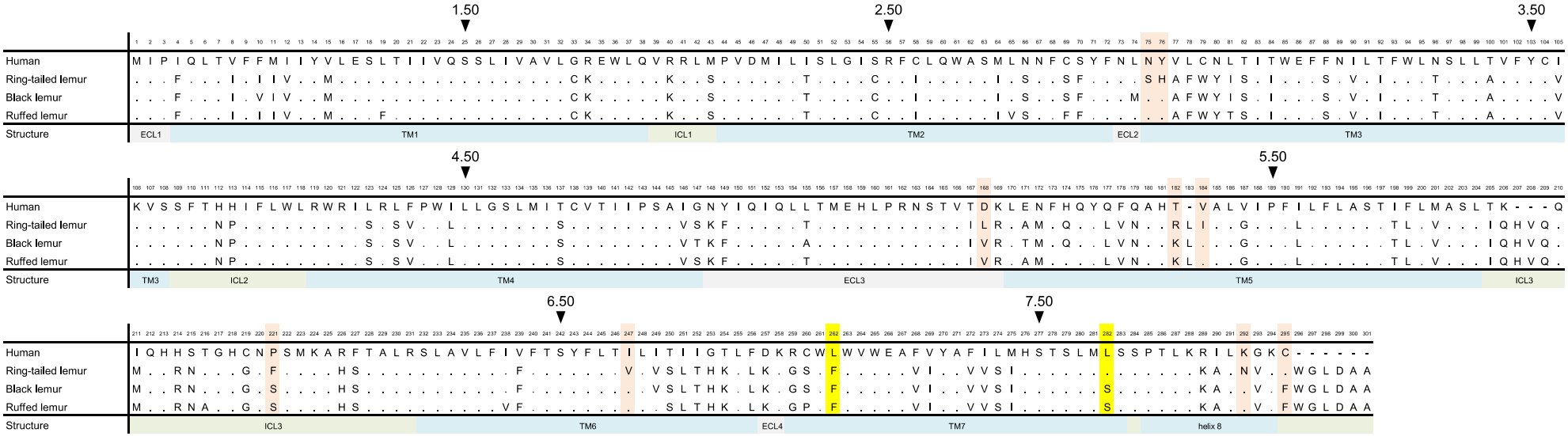

Table S5. Amino acid sequence identities of TAS2R16 among human and three lemurs.

	human	Ring-tailed lemur	Black lemur	Ruffed lemur
human		68.62 %	69.31 %	68.97 %
Ring-tailed lemur			95.02 %	93.69 %
Black lemur				95.35 %
Ruffed lemur				

Table S6. Primers to amplify *TAS2R16* in strepsirrhines and tarsiers

ID	Sequence	Target
sTAS2R16F	TGGGAATAATCAAATCACCT	*TAS2R16* in strepsirrhines
sTAS2R16R	GKTATTGGTATTAATTGCATC	*TAS2R16* in strepsirrhines
tTAS2R16F	CAA ATCACCTCAGGAGMAGGA	*TAS2R16* in tarsiers
tTAS2R16R	GTGTAGACACCATGRTTTTGACTGTC	*TAS2R16* in tarsiers